

Near-infrared studies of the 2010 outburst of the recurrent nova U Scorpii

D. P. K. Banerjee,^{1*} R. K. Das,¹ N. M. Ashok,¹ M. T. Rushton,² S. P. S. Eyres,²
M. P. Maxwell,² H. L. Worters,³ A. Evans⁴ and B. E. Schaefer⁵

¹*Astronomy and Astrophysics Division, Physical Research Laboratory, Navrangapura, Ahmedabad - 380009, Gujarat, India*

²*Jeremiah Horrocks Institute for Astrophysics and Supercomputing, University of Central Lancashire, Preston, PR1 2HE*

³*South African Astronomical Observatory, PO Box 9, 7935 Observatory, South Africa*

⁴*Astrophysics Group, Keele University, Keele, Staffordshire, ST5 5BG*

⁵*Physics and Astronomy, Louisiana State University, Baton Rouge, LA 70803, USA*

Accepted 2010 August 12. Received 2010 August 11; in original form 2010 July 14

ABSTRACT

We present near-infrared (near-IR) observations of the 2010 outburst of U Sco. *JHK* photometry is presented on 10 consecutive days starting from 0.59 d after outburst. Such photometry can gainfully be integrated into a larger data base of other multiwavelength data which aim to comprehensively study the evolution of U Sco. Early near-IR spectra, starting from 0.56 d after outburst, are presented and their general characteristics discussed. Early in the eruption, we see very broad wings in several spectral lines, with tails extending up to $\sim 10\,000\text{ km s}^{-1}$ along the line of sight; it is unexpected to have a nova with ejection velocities equal to those usually thought to be exclusive to supernovae. From recombination analysis, we estimate an upper limit of $10^{-4.64^{+0.92}_{-0.74}} M_{\odot}$ for the ejected mass.

Key words: stars: individual: U Sco – novae, cataclysmic variables – infrared: stars.

1 INTRODUCTION

The well-known recurrent nova (RN) U Scorpii has undergone at least six previous outbursts in 1863, 1906, 1936, 1979, 1987 and 1999, and search of archival data resulted in the detection of three additional outbursts in 1917, 1945 and 1969 (Schaefer 2010). Its latest outburst, on 2010 January 28.4385 UT, was discovered by B. H. Harris and S. Dvorak (Schaefer et al. 2010b).

The latest outburst was predicted to occur around year 2009.3 ± 1 (Schaefer 2005), based on the average brightness and time between eruptions. The binary components of U Sco consist of a massive white dwarf (WD) and a low-mass companion in a 1.2305631 d period eclipsing system (Schaefer & Ringwald 1995). Though the outburst of RNe and classical novae share a common origin in a thermonuclear runaway on a WD surface that has accreted matter from a companion star, an important distinguishing feature in RNe is the smaller amount of accreted mass required and consequently the shorter intervening period to trigger the outburst. Thus RNe are well suited to provide observational inputs and constraints to nova trigger theories (Schaefer 2005). RNe are also of particular interest as they are possibly progenitors of Type Ia supernovae (Starrfield, Sparks & Shaviv 1988; Hachisu et al. 1999).

The last three outbursts of U Sco were well studied, especially in the optical (Barlow et al. 1981; Williams et al. 1981; Sekiguchi et al. 1988; Munari et al. 1999; Anupama & Dewangan 2000; Iijima

2002). The only major IR study of U Sco was during the 1999 outburst by Evans et al. (2001), who obtained spectra between 2.34 and 27.28 d after outburst. An X-ray study of the super-soft phase was also made by Kahabka et al. (1999) for the 1999 eruption. These studies aimed at determining important physical parameters like the mass of the ejecta, spectral type of the secondary and estimating the He abundance among other parameters. The present outburst was widely anticipated and a major worldwide multiwavelength campaign was planned well in advance. As a result extensive data have been collected and preliminary results have been reported in the UV and X-rays from *Swift* (Osborne et al. 2010; Schaefer et al. 2010a; Schlegel et al. 2010a,b) and *Chandra* observations (Orio et al. 2010), in the optical (Anupama 2010) and the infrared (IR; Ashok, Banerjee & Das 2010; Das, Banerjee & Ashok 2010). In this Letter, we present near-IR spectroscopic and photometric data during the early decline phase. The spectra taken 0.59 d after outburst are the earliest to be recorded for this object in the near-IR.

2 OBSERVATIONS

2.1 Mt. Abu

Near-IR observations were carried out in the *JHK* bands at the Mt. Abu 1.2-m Telescope in the early declining phase of the outburst. The comparison star for photometry was SAO 159825 ($J = 8.26$, $H = 7.92$, $K = 7.88$). Spectra in the wavelength range 1.09–2.2 μm were obtained from day 0.56 to day 4.55 at a resolution of ~ 1000 using a near-IR imager/spectrometer with a 256×256 HgCdTe

*E-mail: orion@prl.res.in

Table 1. Photometry of U Sco from Mt. Abu. The mid-time of observations are given in MJD; Δt is time since outburst, taken to be MJD 5224.9385 (2010 January 28.4385 UT; Schaefer et al. 2010b).

MJD	Δt (d)	<i>J</i>	<i>H</i>	<i>K</i>
5225.5286	0.59	7.00 ± .01	6.72 ± .02	6.32 ± .01
5226.5189	1.58	8.05 ± .02	7.88 ± .05	7.33 ± .06
5227.5402	2.60	8.72 ± .06	8.67 ± .06	8.09 ± .04
5228.5349	3.60	9.13 ± .12	9.38 ± .11	8.60 ± .10
5229.5360	4.60	9.79 ± .09	9.82 ± .10	9.27 ± .15
5230.4666	5.53	10.24 ± .11	10.25 ± .12	9.65 ± .08
5231.4829	6.54	11.06 ± .20	10.61 ± .17	9.84 ± .38
5232.4563	7.52	11.38 ± .14	11.23 ± .24	10.23 ± .59
5233.4805	8.54	12.11 ± .15	12.06 ± .29	11.07 ± .33
5234.4823	9.54	12.53 ± .21	11.97 ± .19	11.82 ± .47

Table 2. Spectroscopy of U Sco. Integration time in s, for blue and red grisms for SOFI.

MJD	Δt (d)	Site	<i>J</i>	<i>H</i>	<i>K</i>
5225.4959	0.56	MtA	120	120	150
5226.4820	1.54	MtA	200	180	180
5227.4886	2.55	MtA	–	–	250
5228.4850	3.54	MtA	500	–	500
5229.4845	4.55	MtA	600	500	500
5230.3476	5.41	ESO	360	–	480
5234.3670	9.43	ESO	720	–	960

NICMOS3 array. Spectral calibration was done using OH sky lines and telluric features that register with the stellar spectra. ω^1 Sco (B1V, $T_{\text{eff}} = 25\,400$ K) was chosen as the standard star and observed at similar airmass to U Sco to ensure the ratioing process removes telluric lines. Subsequent reduction of the spectra and processing of the photometric data follow a standard procedure that is described for, e.g. in Naik, Banerjee & Ashok (2009). All data reduction was done using IRAF tasks.

2.2 ESO

IR spectroscopy was obtained at the 3.6-m New Technology Telescope (NTT), using the SOFI IR spectrograph and imaging camera (Moorwood, Cuby & Lidman 1998). Data were obtained on days 5.41 and 9.43 using the blue and red low-resolution grisms, giving a wavelength coverage of 1–2.5 μm at $R \sim 1000$. Flux calibration and the removal of atmospheric features were achieved by dividing the target spectra by the spectra of the standard star HIP 45652 (B9V) on 2010 February 3 (MJD 5230.6). The data were wavelength-calibrated using a Xenon lamp. A log of photometric and spectroscopic observations is given in Tables 1 and 2, respectively.

3 RESULTS

3.1 IR light curves and spectra

The *JHK* light curves are shown in Fig. 1, along with a matching portion of the optical light curve for comparison. The evolution of the near-IR light curve is rather similar to the optical. Since sampling is only on a daily basis, we have interpolated between points to obtain mean (*J*, *H*, *K* averaged) t_2 and t_3 times of 2.4 and 4.0 d, respectively, for the near-IR. However these values are likely to be on the high side as we missed the fast declining stage

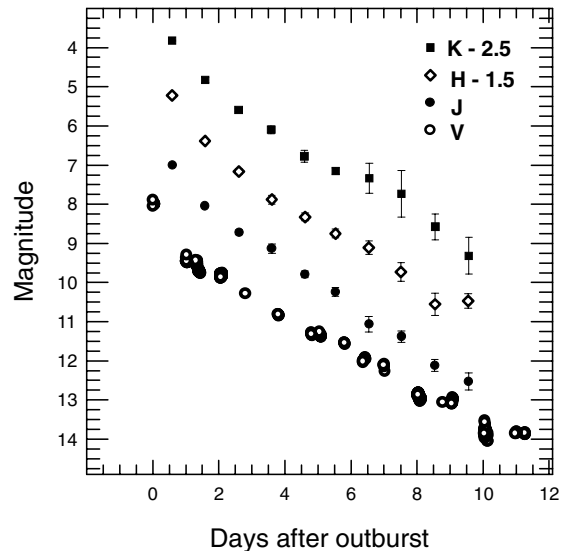


Figure 1. The near-IR and visual light curve of U Sco during the early decline phase. The *V*-band data are from AAVSO. The *J*, *H*, *K* magnitudes have been offset by requisite amounts (as indicated in the figure) for clarity.

between time 0 and 0.59 d (when our first data point was recorded). For the present outburst, Munari, Dallaporta & Castellani (2010) estimate $t_2 = 1.8$ and $t_3 = 4.1$ d in the *V* band. The distance to U Sco as based on t_2 and t_3 has been presented in a unified manner by Schaefer (2010) to be 37.7 kpc, but this is superseded by the blackbody distance of the companion star during the total eclipse, which is 12 ± 2 kpc (Schaefer 2010).

The spectra are presented in Fig. 2. The spectra are similar to those seen in novae outbursts occurring on massive WDs, examples of which are V597 Pup, V2491 Cyg and RS Oph (Banerjee, Das & Ashok 2009; Naik et al. 2009). The prominent features detected in U Sco are the He I 1.0830 μm and Pa γ 1.0938 μm lines (blended), O I 1.1287 μm , Pa β 1.2818 μm , He I 2.0581 μm and the H I Brackett series lines in the *H* band. The Brackett series lines in the *H* band are severely blended due to the large linewidths.

A feature at ~ 1.163 μm is likely N I 1.1625, 1.1651 μm . While this feature also coincides with He II 1.16296, 1.1676 μm , we believe that N I is the more likely: if it is He II, its strength is expected to increase with time, as the level of ionization and excitation increases. While such behaviour is seen for the He I 1.083 and 2.0581 μm lines (Fig. 2), it is not seen for the 1.163 μm feature.

U Sco does not seem to show the presence of prominent carbon lines, and in general C lines are weak in optical spectra during outburst (Barlow et al. 1981; Rosino & Iijima 1988). Carbon emission is a defining IR signature of novae occurring on CO WDs, with mass $\lesssim 1.2 M_{\odot}$ (the so-called ‘CO novae’). Typical spectra of CO novae, and their differences from the present spectra, can be seen in the cases of V2274 Cyg (Rudy et al. 2003), V1280 Sco and V2615 Oph (Das et al. 2008; Das, Banerjee & Ashok 2009). For example, in V2274 Cyg the C I line at 1.44 μm ($^3\text{P}-^3\text{D}$) was comparable in strength with Br γ , but there is no evidence for it in U Sco.

The emission lines are remarkably broad and the H I lines (Pa β and Br γ) consist of a core component and possible broad wings, a detailed discussion of which is given in Section 3.2. The core component has a FWZI in the range of 9000–10 000 km s^{-1} for all the prominent lines. A triple-peaked profile is seen in the Pa β , Br γ and He II 2.058 μm lines in the earliest spectra, 0.56 d after outburst which, however, disappears by the next day (Figs 2 and 3). Similar

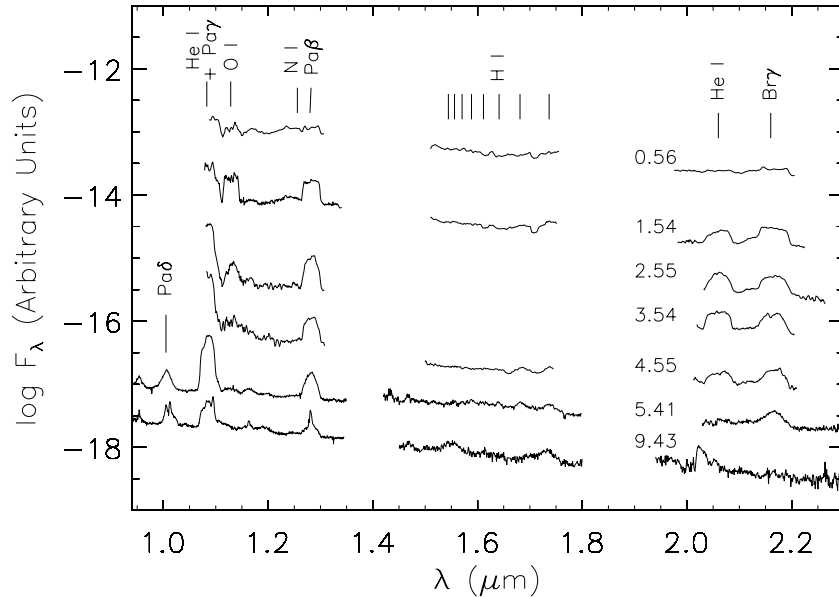


Figure 2. The *JHK* spectra; the time (in days) from outburst is given next to the *K*-band data.

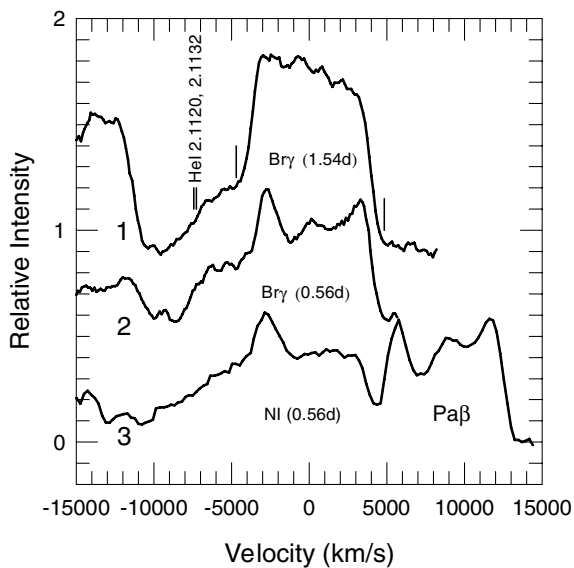


Figure 3. Velocity profiles 1 and 2 are for $\text{Br}\gamma$ on days 1.54 and 0.56, respectively; they have a core component between -4700 and $+4850 \text{ km s}^{-1}$ (marked by lines), and an extended blue wing (see Section 3.2). The expected positions of $\text{He I } 2.1120, 2.1132 \text{ }\mu\text{m}$ lines are shown. Profile 3 is for the $\text{N I } 1.2461, 1.2470 \text{ }\mu\text{m}$ line on day 0.56, which also shows an extended blue wing. The ordinate is in arbitrary units with the profiles offset for clarity.

triple-peaked (‘Batmanesque’) structure was seen in $\text{H}\alpha$ in early optical spectra (Arai et al. 2010). A triple-peaked profile is also seen in the $\text{O I } 1.1287 \text{ }\mu\text{m}$ line on 2010 January 28.996 UT, but we caution that the region around this line has low atmospheric transmission and artificial structures can be generated in the profile during spectrum extraction.

The line fluxes for day 0.56 are given in Table 3.

3.2 Evidence for high-velocity ejecta

The FWHM of the IR emission lines in the 1999 eruption indicated velocities of $\sim 2500 \text{ km s}^{-1}$ (Evans et al. 2001) and FWZI of $\sim 9500 \text{ km s}^{-1}$ over the first five days; likewise the FWZI of the Balmer lines were $\sim 10000 \text{ km s}^{-1}$ in the 1979 (Barlow et al. 1981) and 1999 (Iijima 2002, data obtained on day 0.65, close to our first spectrum) eruptions. Examination of the $\text{Br}\gamma$ profile in the 2010 eruption (Fig. 3) shows a core component with a FWZI of $\sim 9500 \text{ km s}^{-1}$. More interesting however is the very extended blueward wing in the profiles for the first two days, which extend to about 10000 km s^{-1} from the line centre. It is not clear whether an equivalent red wing exists for $\text{Br}\gamma$, as our spectra do not extend that far redward. For the present, we concern ourselves with the 10000 km s^{-1} blueward wing.

We first establish that the extended blue wing of $\text{Br}\gamma$ is genuine and intrinsic to the line by noting that the $\text{N I } 1.2461, 1.2470 \text{ }\mu\text{m}$ lines, also plotted in Fig. 3, exhibit a similar wing. It is difficult

Table 3. Line fluxes (in $10^{-18} \text{ W cm}^{-2}$), dereddened for $E(B - V) = 0.2$.

Day	$\text{O I } 1.1287$	$\text{N I } 1.1625, 1.1651$	$\text{N I } 1.2461, 1.2470$	$\text{P}\beta 1.2818$	$\text{Br}11 1.6806$	$\text{He I } 2.0581$	$\text{Br}\gamma 2.1655$
0.56	5.80 ± 0.17	3.43 ± 0.10	4.50 ± 0.18	4.10 ± 0.18	1.50 ± 0.03	0.59 ± 0.04	2.25 ± 0.08
1.54	10.20 ± 0.10	–	–	9.00 ± 0.20	0.67 ± 0.03	1.33 ± 0.10	$1.93 \pm 0.20 / 2.70 \pm 0.20^*$
2.55	–	–	–	–	–	1.01 ± 0.04	$1.1 \pm 0.05 / 1.35 \pm 0.04^*$
3.54	2.52 ± 0.13	–	–	4.76 ± 0.14	–	0.72 ± 0.04	$0.67 \pm 0.03 / 0.77 \pm 0.03^*$
4.55	–	–	–	1.70 ± 0.07	0.094 ± 0.006	0.24 ± 0.02	$0.31 \pm 0.02 / 0.40 \pm 0.02^*$
5.41	–	–	–	0.73 ± 0.08	0.063 ± 0.005	–	0.17 ± 0.06
9.43	–	–	–	0.058 ± 0.009	–	–	–

*The two values for the $\text{Br}\gamma$ flux are for the core component and for the profile including the blue wing respectively.

to conclude whether other lines have similar wings. Pa β and O I 1.1287 μm are closely flanked on the blue side by other lines. There may be a wing on He I 2.0581 μm as there is a small undulation at $\sim 2.006 \mu\text{m}$, $\sim -7500 \text{ km s}^{-1}$, for first two days (see Fig. 2); a similar ‘bump’ is seen in the 1999 spectrum of Evans et al. (2001). But we again caution that the position of this undulation is in a region of poor atmospheric transmission. Could the wings in Fig. 3 be caused by additional spectral lines? No such line is expected in the case of the N I, but the Br γ wing is the site of the He I 2.1120, 2.1132 μm lines. However the expected positions of these He I lines, marked in Fig. 3, are not too well centred with the extended wing. Thus it is unlikely that they contaminate the wing. Additionally, the He I 2.1120 μm line may be expected to be weaker by a factor of at least 20 compared to He I 2.0581 μm (Benjamin, Skillman & Smits 1999). Observations of other novae (e.g. RS Oph; Banerjee et al. 2009) strongly support this. However, Fig. 3 shows that the strength of the Br γ blue wing, especially in the spectrum 0.56 d after outburst, is too strong compared to He I 2.0581 μm , for it to be caused by the He I 2.1120 μm line. We thus consider it unlikely that there is any significant presence of He I 2.1120 μm and conclude that the broad wing is intrinsic to Br γ and therefore suggestive of material moving at $\sim 10\,000 \text{ km s}^{-1}$; even if this represents the line-of-sight velocity of ejected material, it is well in excess of expected ejecta speeds, even for RNe.

It is possible that this material arises in a bipolar flow. Such bipolar flows have been observed in novae (e.g. RS Oph, V445 Pup; Bode et al. 2007; Woudt et al. 2009), and are explained on the basis of ejected material encountering density enhancements in the equatorial (orbital) plane compared to the polar direction; the outflowing material thus expands more freely in the polar direction, leading to high-velocity polar flows. Such an outflow would be expected to be perpendicular to the orbital plane, and in the case of U Sco (as it is an eclipsing binary with inclination angle $\sim 80^\circ$; (Hachisu et al. 1999), close to the plane of the sky. If we assume inclination $\sim 80^\circ$ and opening angle $\sim 15^\circ$ for the jet, the $10\,000 \text{ km s}^{-1}$ line-of-sight velocity translates to a space velocity of $\sim 23\,000 \text{ km s}^{-1}$. Either way a very fast flow is being witnessed, possibly the fastest seen in any nova eruption.

We note that most of the spectral studies of the 1999 outburst showed the H α profile to have similar broad wings. The doubt again arises whether these are intrinsic to the H α line or caused by additional lines. For example, Iijima (2002), in a spectrum taken 16 h after maximum, assigns the N II line at 6482 \AA as a possible cause for the extended blue wing of the H α profile. However, if it is an intrinsic structure and not really N II 6482 \AA which is contributing, then it is seen that the wing extends to about $10\,900 \text{ km s}^{-1}$ from the line centre (fig. 2 of Iijima 2002). This is in good agreement with the above discussion, and is supporting evidence for a very fast flow.

3.3 Mass estimate using recombination analysis

In the analysis below, we are able to set a useful upper limit on the ejecta mass; an exact determination is difficult due to uncertainty in the conditions in the ejecta and the range of velocities present. For the recombination analysis, we use the data for 2010 February 2.8 (day 5.41); we consider this to be the most favourable epoch, because the lines are more likely to be optically thick at earlier times, while the hydrogen lines for day 9.43 are likely contaminated by He II Pickering lines, which occur at the same wavelengths as the H I lines. We use the best-defined lines from our data for this

epoch, namely Br γ , Pa β and Br 11 (1.6806 μm). The strengths of the other Brackett series lines in the H band are difficult to assess because of blending. We assume there is no significant contribution to the strength of these H I lines from the He II Pickering lines on day 5.41.

We proceed on the assumption that the ejecta are optically thin in the Pa β , Br γ and Br 11 lines. It is expected that nova ejecta have density in the range $n_e = 10^{10} - 10^{12} \text{ cm}^{-3}$ in the early stages. Thus, for example, for $n_e = 10^{11} \text{ cm}^{-3}$ and $T = 10^4 \text{ K}$, case B predicts ratios of 4.76 and 3.8 for Pa β /Br γ and Br γ /Br 11, respectively. The observed ratios in U Sco for Pa β /Br γ (4.29 ± 0.15) and Br γ /Br 11 (2.69 ± 0.80) are reasonably in agreement with these predictions, although there is no plausible combination of n_e and T_e that has the Pa β /Br γ ratio as low as ~ 4.3 (the case B emissivities at $n_e = 10^{11} \text{ cm}^{-3}$, $T = 10^4 \text{ K}$ are 3.1×10^{-26} , 6.5×10^{-27} and $1.7 \times 10^{-27} \text{ erg cm}^3 \text{ s}^{-1}$ for the Pa β , Br γ and Br 11 lines, respectively; Storey & Hummer). If the lines under consideration are largely optically thick, considerable changes are seen in the ratios (especially in the Br γ /Br 11 ratio which can even drop below unity; see Banerjee et al. 2009).

The mass of the emitting gas is given by

$$M = \sqrt{4\pi D^2 m_H^2 (fV/\epsilon)},$$

where D is the distance, m_H the proton mass, f the observed flux in a particular line, ϵ the corresponding case B emissivity; V is the volume of the emitting gas, which is $[(4/3)\pi vt]^3 \phi$, where ϕ , v and t are the filling factor, velocity and time after outburst, respectively. We use $D = 12 \pm 2 \text{ kpc}$ (Schaefer 2010), $v = 5000 \text{ km s}^{-1}$ (although a range of a factor 2 either side of this value is implied by our data) and values of $f = (7.31 \pm 0.01) \times 10^{-12}$, $(1.70 \pm 0.06) \times 10^{-12}$ and $(6.3 \pm 0.2) \times 10^{-13} \text{ ergs s}^{-1} \text{ cm}^{-2}$ measured for the core components of the Pa β , Br γ and Br 11 lines, respectively.

The greatest uncertainty in our analysis arises from our ignorance of the electron density and temperature in the ejecta, and from our assumption that case B applies. If we suppose that $10^8 \leq n_e (\text{cm}^{-3}) \leq 10^{12}$ and $10^4 \leq T_e (\text{K}) \leq 3 \times 10^4$, then the mean $\log \epsilon$ (in $\text{erg s}^{-1} \text{ cm}^3$) is $-25.90^{+0.59}_{-0.32}$, $-26.68^{+0.55}_{-0.35}$ and $-27.23^{+0.46}_{-0.37}$ (Storey & Hummer 1995) for Pa β , Br γ and Br 11, respectively, where the ‘error bars’ represent the range of values. Over this range of n_e and T_e , the case B ratios for Pa β /Br γ and Br 11/Br γ range from 4.8 to 8.4, and 2.7 to 4.5, respectively. As already noted, the observed Pa β /Br γ ratio is less than the lowest value expected for case B, possibly indicating that Pa β may not be optically thin; the mass derived from Pa β may therefore be an underestimate. We find $\log M = 10^{-4.71^{+0.55}_{-0.49}} \phi M_\odot$, $\log M = 10^{-4.64^{+0.53}_{-0.24}} \phi M_\odot$ and $\log M = 10^{-4.58^{+0.51}_{-0.50}} \phi M_\odot$, from Pa β , Br γ and Br 11, respectively. The errors in f , D , v and the uncertainties in ϵ have been added in quadrature, although we recognize that this is not necessarily robust (e.g. the errors are asymmetric (see Barlow 2003, for a discussion of this point), while the uncertainties in ϵ are not in any sense ‘errors’ and are not distributed normally). Our best estimate of the ejecta mass is therefore $10^{-4.64^{+0.92}_{-0.74}} \phi M_\odot$ ($\sim 2.2 \times 10^{-5} \phi M_\odot$), since we must have that $\phi < 1$, $M < 10^{-4.64^{+0.92}_{-0.74}} M_\odot$.

An alternative estimate of the ejected mass can be provided by free-free (f-f) emission (cf. Evans et al. (2001), who found $M \sim$ a few $\times 10^{-7} M_\odot$). We constructed the SED using V magnitudes from AAVSO, our near-IR magnitudes, and reddening $E(B - V)$ in the range 0.2–0.56 (Barlow et al. 1981; Hachisu et al. 2000). We have searched for an f-f excess on the first six days, where the errors on the JHK magnitudes are small. Depending on the reddening, blackbody fits with effective temperatures in the range

6000–8000 K reasonably fit the data. However, while our analysis shows that an f–f excess might be present in the data, especially in the K band, it is marginal and difficult to quantify. In view of this we do not use f–f to estimate a mass. Observations at mid-IR wavelengths should reveal any f–f emission as the emissivity is proportional to λ^2 .

ACKNOWLEDGMENTS

The research at PRL is funded by the Dept. of Space, Government of India. We acknowledge with thanks the use of AAVSO data.

REFERENCES

- Anupama G. C., 2010, *Astron. Telegram*, 2411
 Anupama G. C., Dewangan G. C., 2000, *AJ*, 119, 1359
 Arai A., Yamanaka M., Sasada M., Itoh R., 2010, *Cent. Bureau Electron. Telegrams*, 2152
 Ashok N. M., Banerjee D. P. K., Das R. K., 2010, *Cent. Bureau Electron. Telegrams*, 2153
 Banerjee D. P. K., Das R. K., Ashok N. M., 2009, *MNRAS*, 399, 357
 Barlow R. et al., 1981, *MNRAS*, 195, 61
 Barlow R., 2003, in Lyons L., Mount R., Reitmeyer R., eds, *Particle Physics, Astrophysics and Cosmology*, p. 250, published online at www.conf.slac.stanford.edu/physstat2003
 Benjamin R. A., Skillman E. A., Smits D. P., 1999, *ApJ*, 514, 307
 Bode M. F. et al., 2007, *ApJ*, 665, L63
 Das R. K., Banerjee D. P. K., Ashok N. M., Chesneau O., 2008, *MNRAS*, 391, 1874
 Das R. K., Banerjee D. P. K., Ashok N. M., 2009, *MNRAS*, 398, 375
 Das R. K., Banerjee D. P. K., Ashok N. M., 2010, *Cent. Bureau Electron. Telegrams*, 2157
 Evans A., Krautter J., Vanzi L., Starrfield S., 2001, *A&A*, 378, 132
 Hachisu I., Kato M., Nomoto K., Umeda H., 1999, *ApJ*, 519, 314
 Hachisu I., Kato M., Kato T., Matsumoto K., 2000, *ApJ*, 528, L97
 Iijima T., 2002, *A&A*, 387, 1013
 Kahabka P., Hartmann H. W., Parmar A. N., Negueruela I., 1999, *A&A*, 347, L43
 Moorwood A., Cuby J. G., Lidman C., 1998, *Messenger*, 91, 9
 Munari U. et al., 1999, *A&A*, 347, L43
 Munari U., Dallaporta S., Castellani F., 2010, *Inf. Bull. Var. Stars*, 5930
 Naik S., Banerjee D. P. K., Ashok N. M., 2009, *MNRAS*, 394, 1551
 Orio M. et al., 2010, *Astron. Telegram*, 2451
 Osborne J. et al., 2010, *Astron. Telegram*, 2442
 Rosino L., Iijima T., 1988, *A&A*, 201, 89
 Rudy R. J. et al., 2003, *ApJ*, 596, 1229
 Schaefer B. E., 2005, *ApJ*, 621, L53
 Schaefer B. E., 2010, *ApJS*, 187, 275
 Schaefer B. E., Ringwald F. A., 1995, *ApJ*, 447, L45
 Schaefer B. E. et al., 2010a, *Astron. Telegram*, 2452
 Schaefer B. E. et al., 2010b, *AJ*, 140, 925
 Schlegel E. M. et al., 2010a, *Astron. Telegram*, 2419
 Schlegel E. M. et al., 2010b, *Astron. Telegram*, 2430
 Sekiguchi K. et al., 1988, *MNRAS*, 234, 281
 Starrfield S., Sparks W. M., Shaviv G., 1988, *ApJ*, 325, L55
 Storey P. J., Hummer D. G., 1995, *MNRAS*, 272, 41
 Williams R. E. et al., 1981, *ApJ*, 251, 221
 Woudt P. A. et al., 2009, *ApJ*, 706, 738

This paper has been typeset from a $\text{\TeX}/\text{\LaTeX}$ file prepared by the author.